Experimental Study on the Mechanical Behaviors of PVA-ECC after Freeze-Thaw Cycles

Wenjie Ge[1,2]*, Chen Cai[1], Xiang Ji[1], Ashraf F Ashour[2], BiYuan Wang[1]

[1] College of Civil Science and Engineering, Yangzhou University, YangZhou, 225127, China; gewj@yzu.edu.cn
[2] School of Engineering, University of Bradford, Bradford, West Yorkshire, BD7 1DP, UK; a.f.ashour@bradford.ac.uk.

Abstract: In order to study the mechanical behaviors of engineered cementitious composites (ECC) reinforced with various types of polyvinyl alcohol (PVA) fibers and different fiber volume fractions after the freeze-thaw cycles, the rapid freeze-thaw method was used to test the mass loss ratios, longitudinal relative dynamic elastic modulus, compressive strength and flexural strength. The results showed that specimens incurred more serious damage with the increasing of freeze-thaw cycles; however their performance would be improved by fiber type and dosage. Mass loss rate of JPA (specimen with 2% volume content of JP fiber) was lower than JPB (specimen with 1% volume content of JP fiber). Furthermore, the mass loss rate of JPB was lower than that of CPB (specimen with 1% volume content of CP fiber). The longitudinal relative dynamic elastic modulus of JPA was higher than that of JPB while the longitudinal relative dynamic elastic modulus of JPB was higher than that of CPB. In addition, the compressive strength and flexural strength decreased with the increasing of freeze-thaw cycles. Mechanical behaviors of specimens with fiber exhibited better strength than specimens without fiber. Based on the SL 211-2006 code for the design of hydraulic structures against ice and freezing action, JPA and JPB specimens are adequate for use in severe cold regions, while specimen CPA and CPB can be used in cold regions, specimen JPC only can be used in warm regions.

Keywords: ECC; PVA fibers; Freeze-thaw cycles; Mass loss rate; Relative dynamic elastic modulus; Compressive strength; Flexural strength

Introductions

Normal concrete inherently has the characteristics of low tensile strength, poor toughness, high self-weight and poor crack resistance. In order to overcome some of the above shortcomings, Li [1-3] incorporated PVA fiber into the cement mortar to produce ECC. By adding up to 2.0% volume content of PVA fiber, selecting suitable cementitious materials and additives, ECC can be produced with ultimate tensile strain higher than 3.0%, high toughness, impact resistance and strain hardening performance.

ECC is a new generation of high performance fiber reinforced cementitious composite featuring high ductility and medium fiber content. The tensile strain capacity in the range of 3.0% to 5.0% has been demonstrated in ECC materials by using polyethylene fibers or PVA fibers with fiber volume fraction less than 2.0%. Large strain is achieved by sequential development of multiple cracks, instead of continuous increasing of the crack opening. The associated high fracture toughness and controlled crack width (typically below 100 μm) make ECC an ideal material to improve both the serviceability and the durability of infrastructures. Typical characteristics of ECC tested by our research group are shown in Figure 1[4]. Recently, the application fields of ECC have increased, for example it has been successfully applied to dam repairing, bridge deck overlays, coupling beams in high rise buildings and

other structural elements and systems.

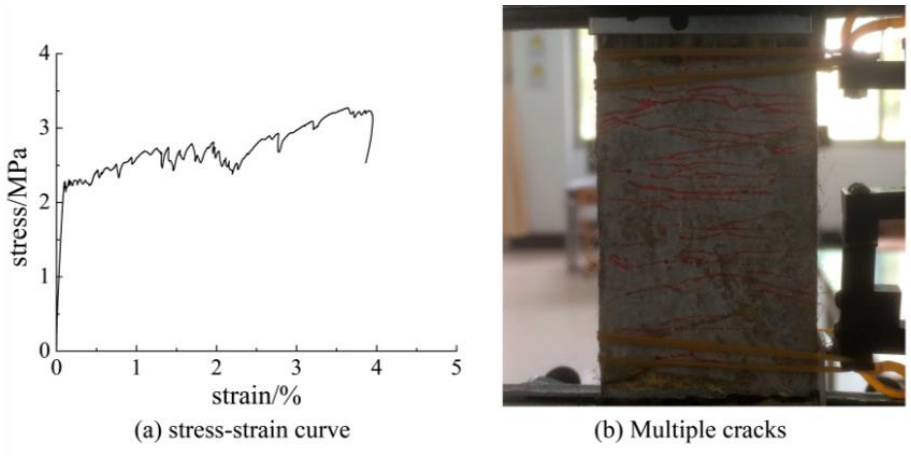

Fig.1 Typical characteristics of ECC

In order to encourage the use of ECC material in cold regions, such as northern Europe, Canada, northern United States, Russia and north China, the mechanical behaviors and frost resistance of ECC have been investigated by many scholars. Recent studies showed that ECC exhibited tensile strain hardening and multiple cracking performances regardless of the proportion [5], type of fibers[6, 7] (PVA fibers made by different manufacturers, non-round polypropylene fiber and low modulus polyvinyl alcohol fiber)), strain rate loading [8] and water to binder ratio varying from 0.55 to 0.25[9]. ECC had also adequate compressive performance with different mix proportions [10] or water to binder ratio [9]. Previous experimental studies showed that ECC continued to demonstrate strain hardening and multiple cracking after freeze-thaw cycles [11, 12]. The dynamic elastic modulus had no obvious decrease after 300 freeze-thaw cycles [5, 12]. The ultimate strain of ECC was still higher than 3.0% and the frost resistance of ECC met the requirement of most structures [13]. ECC's ultimate strain was still higher with different content of fly ash and PVA fibers after freeze-thaw cycles [12, 14-16]. Frost resistant grades of ECC with different types of fibers and gray-sand ratios were higher than F300 [12, 17-18] (Specimens are considered to failure [19] when the longitudinal relative dynamic elastic modulus has decreased to 60.0% of its initial value or its mass loss rate has exceeded 5.0%) and it can be used in cold regions. Self-healing ability and durability of ECC decreased significantly after freeze-thaw cycles in chloride environment compared to fresh water environment [20, 21].

Most previous investigations were conducted on the mechanical behavior of ECC with Kuraray PVA fibers. Since the mechanical behavior of ECC may be significantly influenced by the type of fibers and mixtures [6, 7], research on the mechanical behavior of ECC with different types of fibers and mixtures after freeze-thaw cycles are necessary to promote the use of ECC in cold regions. In this study, PVA fibers produced by two different sources were investigated to compare the experimental results on mass loss ratios, longitudinal relative dynamic elastic modulus, compressive strength and flexural strength after being subjected to freeze-thaw cycles.

1 EXPERIMENTS PRLGRAM

1.1 Test Materials

Portland cement produced by LvYang Cement Corporation was utilized. Grade I fly ash, superfine silica fume, 100-200 mesh special fine quartz sand and Sika poly acid water reducer were also used. RECS15*12 type PVA fiber and type II PVA fiber were utilized. The properties of fibers are shown in Table1, in which JP means RECS15*12 type PVA fiber and CP means type II PVA fiber. Test materials are shown in Figure 2.

Table 1 The properties of fibers

Fiber type	Length /mm	Diameter /μm	Elastic modulus / GPa	Elongation / %	Tensile strength / ($N \cdot mm^{-2}$)	Density / (g/cm^3)
JP	12	40	41	6.5	1560	1.3
CP	12	20	37	6	1300	1.3

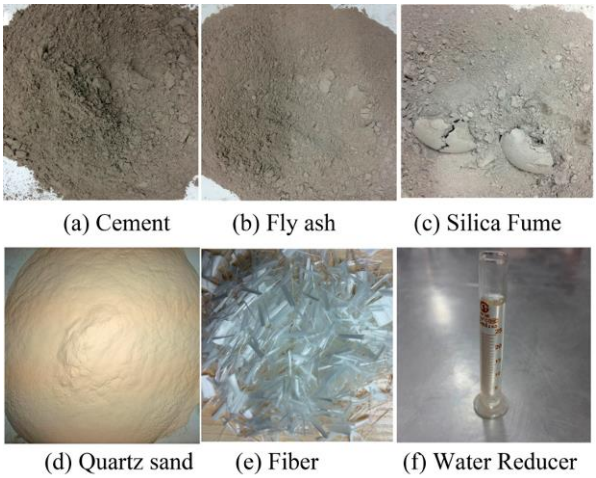

Fig.2 Test materials

1.2 Experimental Design

Fiber post-addition method was adopted in the mixing procedure [22]. First, cement, fly ash, silica fume, sand and other dry ingredient were added to the mixture and they were mixed for one minute at the speed of 60 rpm to distribute the mixture uniformly. HJS-60 twin shafts concrete mixer was used (as shown in Figure 3(a)). Then, water was added and the mixture was mixed for another one minute at the same speed. Water reducer was then added until the mortar has shown sufficient fluidity, and the mixture was mixed two more minutes at the speed of 120 rpm until the cement mortar could self level when stopping the mixing, as shown in Figure 3(b). Fiber was then added, and the mix was stirred for another 3~6 minutes at the speed of 120 rpm. ECC was poured into molds that were vibrated (as shown in Figure 3(c)) for 2 minutes for sufficient compaction. After smoothing the surface, the molds were covered with transparent plastic film to prevent evaporation. Formworks were demolded after 24-hours natural indoor temperature curing, and then specimens were placed in the standard curing room having a controlled temperature of 20±2 ^{o}C and relative humidity of over 95% for 28 days.

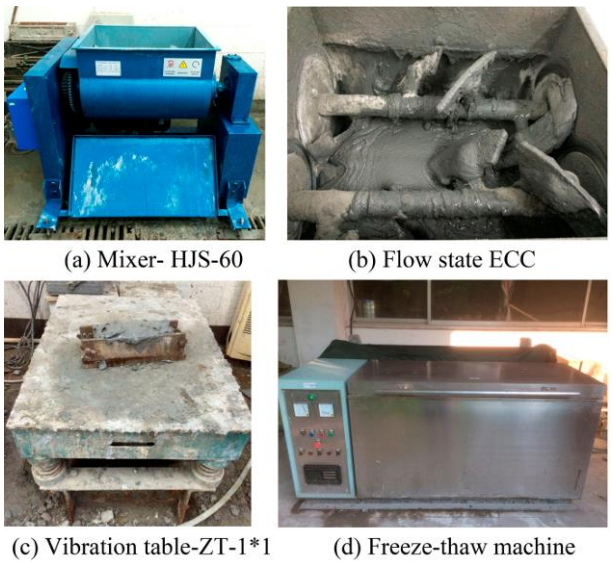

Fig.3 Testing Machines

Uniform fiber distribution was achieved by adjusting the ratio of fly ash, the amount of water reducer

and functional constituents [22]. Mixture ratios of ECC are shown in Table 2. Mass ratio of cement, fly ash, silica fume, sand and water were 1.0:3.0:1.0: 0.36:0.3 respectively. JPA and JPB represent specimens with 2.0% and 1.0% volume content of JP fiber, respectively, CPA and CPB represent specimens with 2.0% and 1.0% volume content of CP fiber, respectively, whereas JPC indicates specimen without fiber as shown in Table 2.

Table 2 ECC mixture ratio

Serial number	Water reducer/%	PVA volume Fraction/%	Fiber distribution	Fiber type
JPA	0.48	2.0	uniform distribution	JP
JPB	0.44	1.0	uniform distribution	JP
JPC	0.21	0.0	-	-
CPA	0.57	2.0	slight uneven distribution	CP
CPB	0.52	1.0	uniform distribution	CP

1.3 Freeze-thaw cycle test

According to test code for hydraulic concrete SL 352-2006 [19], rapid water freeze-thaw cycles method was adopted. The minimum and maximum temperatures of the specimen centers should be controlled at -17±2 ^{o}C and 6±2 ^{o}C respectively. Each full freeze-thaw cycle should be completed in about 3 hours. Rapid freeze-thaw automatic test equipment CDR2, as shown in Figure 3 (d), produced by YanXin Technology Corporation was used. 40 mm × 40 mm × 160 mm prism specimens were used to test the mass loss rate, longitudinal relative dynamic elastic modulus and flexural strength. 70.7 mm × 70.7 mm × 70.7 mm cube specimens were used to assess the compressive strength. Mass loss rate, longitudinal relative dynamic elastic modulus, compressive strength and flexural strength were measured after every 25 freeze-thaw cycles.

According to the standard for test method of basic properties of construction mortar JGJ/T 70-2009 [23], unfrozen specimens were also made and stored in the standard curing room in a similar conditions to these subjected to freeze-thaw cycles for comparison. Compressive test and flexural test were made (before tests were conducted, the comparison specimen were submerged in water). Test of freeze-thaw specimens and comparison specimens were conducted at the same time.

2 TEST RESULTS AND ANALYSIS

2.1 Failure Modes

Specimens were smooth with no crack or holes on their surface before freeze-thaw cycles. Specimen CPA exposed small amount of fibers on its surface after 200 freeze-thaw cycles and showed slight loss of mortar. Specimen JPB incurred cracks on its surface after 200 freeze-thaw cycles and mortar dropped slightly. Though much fiber was exposed on the surface of specimen JPA after 200 freeze-thaw cycles, there was a slight mortar loss. After 200 freeze-thaw cycles, specimen JPC incurred serious damage, with spalling on its surface. CPB also incurred motor spalling, but slightly less than JPC because of the connection function of fibers. Specimens after 200 freeze-thaw cycles are shown in Figure 4.

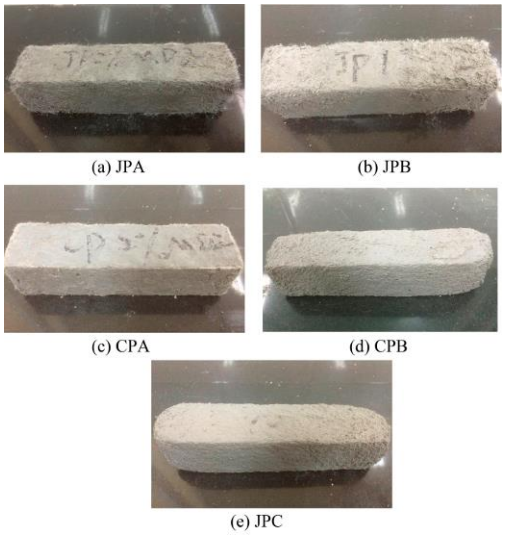

Fig.4 Specimens after 200 freeze-thaw cycles

2.2 Mass Loss Rate

Electronic balance YP6000N with measurement accuracy of 1 g was used to test mass loss rate. Relationships between mass loss rate and freeze-thaw cycles are shown in Figure 5, where R_m is mass loss rate of specimen and it equals the mass of specimen after freeze-thaw cycles to the mass of unfrozen specimen.

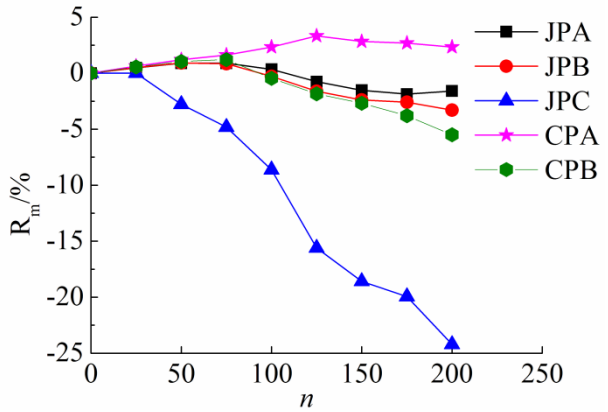

Fig.5 Mass loss ratios

Fig.6 Longitudinal fundamental frequency testing device

As illustrated in the figure, specimen JPC incurred serious mass loss and its value exceeded 5% after 100 freeze-thaw cycles and approached 25% after 200 freeze-thaw cycles. Specimen CPA did not incur mass loss after freeze-thaw cycles. It is believed that water penetrated into the holes formed by the uneven fiber distribution and caused the mass increase of CPA specimen [22]. For specimens JPA and JPB, their mass decreased gradually with the increasing of freeze-thaw cycles, and their mass loss rate were smaller than 5% after 200 freeze-thaw cycles. For specimens with the same types of fiber, mass loss rate of specimen with higher fiber volume content (JPA) was lower than specimen with lower fiber volume content (JPB). In addition, for specimens with the same fiber volume content, mass loss rate of specimen with JP fiber (JPB) was lower than specimen with CP fiber (CPB).

When the PVA fiber volume content is too high, plenty of bubbles would be brought into the cement-based composites [22], leading to the formation of a number of holes. While the holes formed by the uneven fiber distribution and the bubbles were filled with water, mass loss rate of specimens with slight uneven fiber distribution (CPA) is lower than the other specimens.

2.3 Longitudinally Relative Dynamic Elastic Modulus

Longitudinal relative dynamic elastic modulus can be calculated by following formula (1) [19]:

$$R_{Ed}=f_n^2/f_0^2\times100 \quad (1)$$

where R_{Ed} is the longitudinal relative dynamic elastic modulus (%) of specimen after n freeze-thaw cycles, f_n is longitudinal fundamental frequency (Hz) after n freeze-thaw cycles and f_0 is longitudinal fundamental frequency (Hz) of unfrozen specimen. Longitudinal relative dynamic elastic modulus test equipment DT20 with measurement accuracy of 1 Hz was used and is shown in Figure 6. Relationships between longitudinal relative dynamic elastic modulus and freeze-thaw cycles are presented in Figure 7.

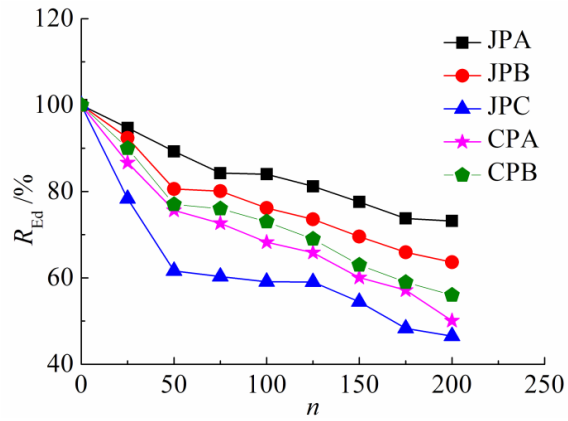

Fig.7 Longitudinal relative dynamic elastic modulus

Fig.8 Compressive test

As depicted from Figure 7, the longitudinal relative dynamic elastic modulus of specimen JPC was lower than 60% of initial value after 100 freeze-thaw cycles, and decreased to 46% of initial value after 200 freeze-thaw cycles. The decrease rate of longitudinal relative dynamic elastic modulus of specimen CPA was lower than that of specimen JPC with the same freeze-thaw cycles. Longitudinal relative dynamic elastic modulus of specimen JPA decreased to 80% of initial value after 150 freeze-thaw cycles and to 50% of initial value after 200 freeze-thaw cycles. The longitudinal relative dynamic elastic modulus of specimen JPA and JPB decreased to 70% of its initial value after 200 freeze-thaw cycles. For specimens with the same fiber type, longitudinal relative dynamic elastic modulus of specimens with higher volume content (JPA) was higher than that of specimen with lower volume content (JPB). In addition, for specimens with the same fiber volume content, longitudinal relative dynamic elastic modulus of specimen with JP fiber (JPB) was higher than that of specimen with CP fiber (JPB).

Longitudinal relative dynamic elastic modulus of specimen with slight uneven fiber distribution (CPA) was lower than that of other specimens. The holes formed by the uneven fiber distribution and bubbles had a deteriorating effect on specimens.

Specimen is considered to reach failure when the longitudinal relative dynamic elastic modulus decreased to 60% of initial value or its mass loss rate exceeded 5%. The corresponding freeze-thaw cycles at this condition is defined as the specimens' frost resistant grade [19]. Mass loss rate of specimens JPA and JPB were smaller than 5% after 200 freeze-thaw cycles and its longitudinal relative dynamic elastic modulus was larger than 60% of initial value. Mass loss rate of specimen JPC was larger than 5% after 100 freeze-thaw cycles and its longitudinal relative dynamic elastic modulus was lower than 60% of initial value. For CPA specimen, its longitudinal relative dynamic elastic modulus was lower than 60% of initial value after 175 freeze-thaw cycles. For CPB specimen, its longitudinal relative dynamic elastic modulus was lower than 60% of initial value after 200 freeze-thaw cycles. The frost resistant grades of each specimen are shown in Table 3.

Table 3 Specimens frost resistant grade

Specimen	Frost resistant grade

JPA	$F_{JPA}>F200$
JPB	$F_{JPB}>F200$
JPC	$F75<F_{JPC}<F100$
CPA	$F150<F_{CPA}<F175$
CPB	$F175<F_{CPB}<F200$

According to the code for design of hydraulic structures against ice and freezing action SL 211-2006 [13], JPA and JPB can be used in severe cold regions where average temperature of coldest month is below -10 °C. Furthermore, CPA and CPB can be used in cold regions where average temperature of coldest month is between -10 °C and -3 °C, and JPC only can be used in mild regions where average temperature of coldest month is higher than -3 °C.

2.4 Compression Performance

Computer controlled automatic pressure testing machine YAW3000C (as shown in Figure 8) was used to measure the compressive strength at the load rate of 1.5 kN/s and accuracy of 0.1 MPa. Compressive strength of specimens after freeze-thaw cycles are shown in Table 4, and relative compressive strengths are shown in Figure 9, where $f_{c,f}$ is compressive strength of specimen after certain freeze-thaw cycles, $f_{c,u}$ is compressive strength of unfrozen specimen with the same curing time as freeze-thaw specimen, $R_{c,1}$ is relative compressive strengths to original strength before freeze-thaw cycles, $R_{c,1}=f_{c,f,n}/f_{c,f,0}$, $R_{c,2}$ is relative compressive strengths to comparison specimen strength, $R_{c,2}=f_{c,f,n}/f_{c,u,n}$.

Table 4 Compressive strength/ ($N\cdot mm^{-2}$)

Specimen		Number of freeze-thaw cycles								
		0	25	50	75	100	125	150	175	200
JPA	$f_{c,f}$	65.4	65.6	63.5	56.7	55.5	54.8	54.3	52.4	50.7
	$f_{c,u}$	65.4	67.0	73.0	75.0	76.5	76.6	79.3	80.7	86.0
JPB	$f_{c,f}$	60.2	60.7	57.7	53.8	52.6	51.1	49.9	46.1	40.5
	$f_{c,u}$	60.2	65.0	72.5	73.2	73.6	73.8	74.7	75.5	85.4
JPC	$f_{c,f}$	51.5	55.0	43.5	36.6	33.8	29.5	28.1	26.7	12.4
	$f_{c,u}$	51.5	58.2	60.8	62.6	63.2	68.7	73.1	73.5	73.7
CPA	$f_{c,f}$	37.7	41.1	39.1	37.4	36.4	34.5	33.6	32.7	31.0
	$f_{c,u}$	37.7	44.0	43.5	47.0	48.2	48.6	50.9	51.0	54.0
CPB	$f_{c,f}$	40.0	41.2	36.8	34.8	34.0	32.8	31.6	29.2	26.0
	$f_{c,u}$	40.0	43.8	47.2	49.7	52.3	54.7	56.4	56.2	61.9

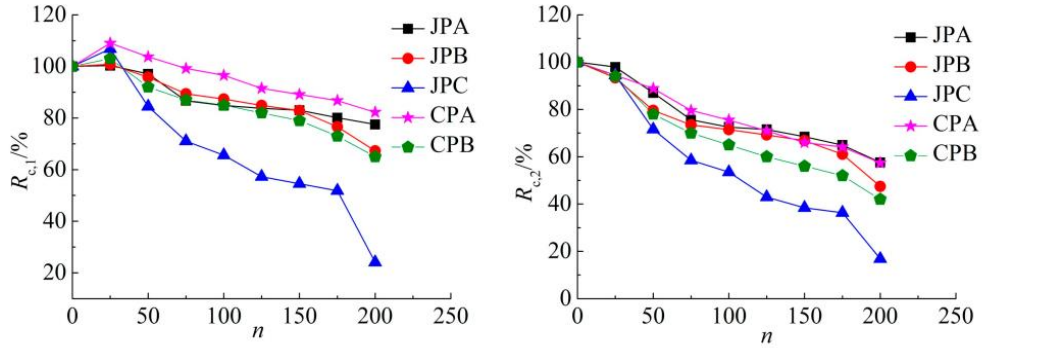

(a) Comparison with unfrozen specimen (b) Comparison with specimen with the same curing age

Fig.9 Compressive strength contrast

As can be seen from Table 4 and Figure 9, compressive strengths of unfrozen specimens increased with increasing fiber content. Compressive strength of specimen CPA was lower than specimen JPC at early stage which could be attributed to its uneven fiber distribution. However its compressive strength became gradually higher than specimen JPC with the increasing of freeze-thaw cycles. The compressive strength of comparison specimen increased with the increasing of curing age. Compressive strengths decreased with increasing of freeze-thaw cycles. Strength decrease rate of

specimen JPC (cement mortar without fiber) was faster than the other groups (specimen incorporated fiber), and its compressive strength after 200 freeze-thaw cycles decreased to 20% of initial strength.

According to the theory of compressive strength of composites [22], the compressive strength of composite is increased with the increasing of fiber modulus. Therefore, with the same fiber volume content, compressive strength of specimens reinforced with JP fiber is expected to be higher than that of specimen reinforced with CP fiber.

2.5 Flexural Test

Electronic universal test machine DNS100 (as shown in Figure 10) was used to conduct 3-point flexural test at the load speed of 1.5 mm/s and accuracy of 0.1 MPa. Flexural strengths of specimens after freeze-thaw cycles are shown in Table 5, and relative flexural strengths are presented in Figure 11, where $f_{f,f}$ is flexural strength of specimen after certain freeze-thaw cycles, $f_{f,u}$ is flexural strength of unfrozen specimen with the same curing time with freeze-thaw specimen, $R_{f,1}$ is relative flexural strength to original strength before freezing, $R_{f,1}=f_{f,f}/f_{f,f,0}$, $R_{f,2}$ is relative flexural strength to strength of comparison specimen, $R_{f,2}=f_{f,f}/f_{f,u}$.

Fig.10 Flexural test

Table 5 Flexural strength/ ($N \cdot mm^{-2}$)

Specimen		number of freeze-thaw cycles								
		0	25	50	75	100	125	150	175	200
JPA	$f_{f,f}$	18.5	17.8	17.3	17.1	16.8	16.7	16.0	15.1	12.6
	$f_{f,u}$	18.5	18.8	19.6	19.8	20.0	20.2	21.0	21.3	21.5
JPB	$f_{f,f}$	12.3	12.0	11.9	11.7	11.1	9.1	9.0	8.8	8.7
	$f_{f,u}$	12.3	12.4	12.5	12.6	12.8	13.0	13.4	13.8	13.9
JPC	$f_{f,f}$	5.9	5.3	4.9	4.4	3.9	3.8	3.5	2.9	2.5
	$f_{f,u}$	5.9	5.9	6.0	6.2	6.5	6.7	6.8	6.8	7.2
CPA	$f_{f,f}$	9.6	9.2	9.0	8.8	8.5	8.1	7.8	7.7	7.6
	$f_{f,u}$	9.6	9.6	9.7	9.7	9.8	9.8	9.9	10.0	10.1
CPB	$f_{f,f}$	8.5	8.0	7.5	7.0	6.6	6.0	5.5	5.1	4.9
	$f_{f,u}$	8.5	8.5	8.8	8.9	9.0	9.0	9.1	9.1	9.2

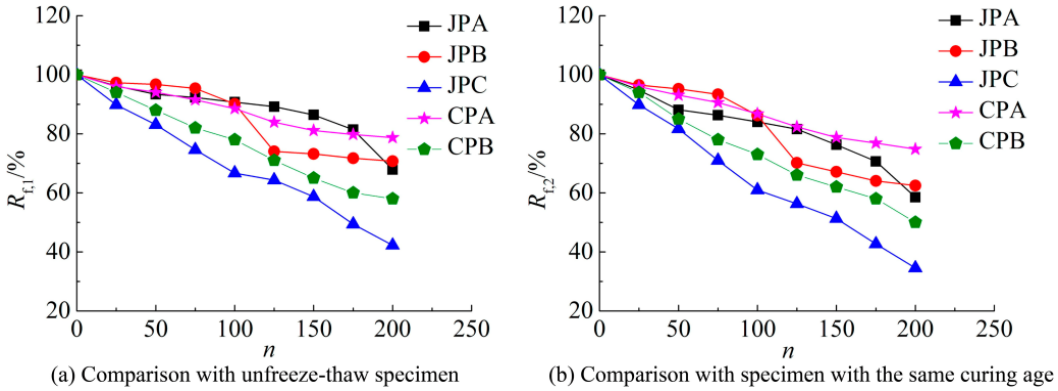

(a) Comparison with unfreeze-thaw specimen (b) Comparison with specimen with the same curing age

Fig.11 Flexural strength contrast

As can be seen from Table 5 and Figure 11, flexural strengths of unfrozen specimen increased with the increasing of fiber content. Due to the uneven fiber distribution, flexural strength of specimen CPA was lower than specimen JPB. Flexural strength of specimen increased with the increasing of curing age but a lower rate than that of compressive strength. Flexural strength decreased with the increasing of freeze-thaw cycles. Strength decrease rate of specimen JPC (cement mortar without fiber) was faster than that of other groups (specimens incorporated fiber).

For specimens with the same types of fiber, flexural strength of specimen with higher fiber volume content are normally than that of specimen with lower fiber volume content. The addition of PVA fibers is beneficial to delaying the occurrence of cracks, controlling the development of cracks and reducing the width of cracks in the flexural specimen [22]. Its effectiveness depends on whether the fibers are broken or pulled out from the matrix. This is influence by the bond between the fiber and the substrate and the tensile strength of the fiber. Generally, the higher the fiber volume contents, the stronger its ability of resisting cracking.

Since PVA fibers has the characteristic of hydrophilic nature and its surface was not treated (CP fiber) [6], CP fibers were easier to fracture because its interface with the matrix produces excessive chemical bond and friction bond. Specimen with JP fiber exhibited good strain-hardening and multiple crack propagation likely because JP fiber' surface was treated.

3 CONCLUSIONS

Experimental results of mass loss rate, relative longitudinal dynamic elastic modulus, compressive strength and flexural strength of specimens with different types of fiber and different volume fraction of fiber were presented. Conclusions are obtained as follows:

1) Specimens incurred more damage with the increasing of freeze-thaw cycles. Specimen without fiber suffered the largest loss of surface and edges. Specimens with fiber can retain their shape. Specimens' performance can be improved by the incorporation of certain fiber.

2) For specimens with the same types of fiber, mass loss rate of specimen JPA with higher volume content was lower than specimen JPB with lower volume content. On the other hand, for specimen with the same fiber volume content, mass loss rate of specimen with JP fiber (JPB) was lower than specimen with CP fiber (CPB).

3) For specimen with the same types of fiber, longitudinal relative dynamic elastic modulus of specimen with higher volume content (JPA) was higher than that of specimen with lower volume content (JPB). For specimen with the same fiber volume content, longitudinal relative dynamic elastic modulus of specimen with JP fiber (JPB) was higher than that of specimen with CP fiber (CPB).

4) Compressive strength and flexural strength of specimens with fiber decreased gradually with increasing freeze-thaw cycles. Strength of specimen without fiber decreased faster and nearly

diminished after 200 freeze-thaw cycles. Specimens with 1% fiber volume fraction exhibited higher strength reduction than those with 2% fiber volume fraction. With the same volume fraction of fiber, strength decrease of specimen with JP fiber was lower than specimen with CP fiber.

5) According to the frost resistant grade for hydraulic structures, specimens with JP fiber were higher than F200 and can be used in severe cold regions. Frost resistant grades of specimen with CP fiber were higher than F150 and can be used in cold regions. Specimen without fiber only can be used in warming regions.

ACKNOWLEDGEMENT

The authors appreciate the support of the National Natural Science Foundation of China (51678514, 51308490), Six Talent Peaks Project of Jiangsu Province (JZ-038, 2016), the Natural Science Foundation of Jiangsu Province, China (BK20130450) and the Jiangsu Government Scholarship for Overseas Studies. Thanks for the comments made by reviewers and editors.

REFERENCE

[1] Victor C Li, Christopher K Y Leung. Steady state and multiple cracking of random discontinuous fiber reinforced brittle matrix composites [J]. Journal of Engineering Mechanics, 1992. 118(11):2246-2264.

[2] Mohamed Maalej, Victor C Li. Introduction of strain-hardening engineered cementitious composites in design of reinforced concrete flexural members for improved durability [J]. ACI Structural Journal, 1995, 92(2): 167-176.

[3] Victor C Li, Shuxin Wang, Cynthia Wu. Tensile Strain-Hardening Behavior of Polyvinyl Alcohol Engineered Cementitious Composite (PVA-ECC) [J]. ACI Journal of Materials, 2001, 98(6): 483-492.

[4] Biyuan Wang, Wenjie Ge, Jingjing Zhou, Dafu Cao. Preparation and mechanic behaviors of engineered cementitious composites [J]. Journal of Yangzhou University (Natural Science Edition), 2015, 18(3): 64-69.

[5] Michael D Lepech, Victor C Li. Long term durability performance of engineered cementitious composites [J]. Restoration of Building and Monuments, 2006, 12(2): 119-132.

[6] Zuanfeng Pan, Chang Wu, Jianzhong Liu, Wei Wang, Jiwei Liu. Study on mechanical properties of cost-effective polyvinyl alcohol engineered cementitious composites (PVA-ECC) [J]. Construction and Building Materials, 2015(78): 397-404.

[7] Parkravan Hamid Reza, Jamshidi Masoud, Latifi Masoud. Study on fiber hybridization effect of engineered cementitious composites with low- and high-modulus polymeric fibers [J]. Construction and Building Materials, 2016, 112: 739-746.

[8] Hedong Li, Shilang Xu. Rate dependence of ultra high toughness cementitious composite under direct tension [J]. Journal of Zhejiang University-SCIENCE A (Applied Physics & Engineering), 2016, 17(6): 417-426.

[9] Jiajia Zhou, Jinlong Pan, Christopher K Y Leung. Mechanical Behavior of Fiber-Reinforced Engineered Cementitious Composites in Uniaxial Compression [J]. Journal of materials in civil engineering, 2015, 27(1): 04014111(1-10).

[10] Jun Zhang, Chengxu Gong, Zili Guo, XianchunJu. Mechanical Performance of Low Shrinkage Engineered Cementitious Composite in Tension and Compression [J]. Journal of Composite Materials, 2016, 43(22): 2571-2585.

[11] Shilang Xu, Xinhua Cai, Hedong Li. Experimental study of the durability properties of ultra-high toughness cementitious composites under freezing and thawing cycles [J]. China Civil

Engineering Journal, 2009, 42(9): 42-46.

[12] Seok-Joon Jang, Keitetsu Rokugo, Wan-Shin Park, et al. Influence of rapid freeze-thaw cycling on the mechanical properties of sustainable strain-hardening cement composite (SSHCC) [J]. Materials, 2014, 7(2): 1422-1440.

[13] China water northeastern investigation, design & research Co., Ltd. Code for Design of Hydraulic Structures against Ice and Freezing Action SL 211-2006 [S]. Beijing: China Water & Power Press, 2006.

[14] Mustafa Sahmaran, Erdog˘an Özbay, Hasan E Yücel, et al. Frost resistance and microstructure of engineered cementitious composites: influence of fly ash and micro poly-vinyl-alcohol fiber [J]. Cement & Concrete Composites, 2012, 34(2): 156-165.

[15] Hyun-Do Yun, Keitetsu Rokugo. Freeze-thaw influence on the flexural properties of ductile fiber-reinforced cementitious composites (DFRCCs) for durable infrastructures [J]. Cold Region Science and Technology, 2012, 78(4): 82-88.

[16] Hyun-Do Yun. Effect of accelerated freeze–thaw cycling on mechanical properties of hybrid PVA and PE fiber-reinforced strain-hardening cement-based composites (SHCCs) [J]. Composites Part B: Engineering, 2013, 52(4): 11-20.

[17] Zongcai Deng, Huiqing Xue, Haibin Xu. Experimental study of durability properties of high toughness fiber reinforced cementitious composites under freezing and thawing cycles [J]. Journal of North China Institute of Water Conservancy and Hydroelectric Power, 2013, 34(1): 16-19.

[18] Zhangu Ju, Shuguang Liu, Changwang Yan, et al. Influence of Chloride environment on frost resistance of PVA Fiber reinforced engineered cementitious composite [J]. Journal of the Chinese Ceramic Society, 2013, 41(6): 766-771.

[19] China renewable energy engineering institute. Test code for hydraulic concrete SL 352-2006 [S]. Beijing: China Water & Power Press, 2006.

[20] Yu Zhu, Yingzi Yang, Yan Yao. Autogenous self-healing of engineered cementitious composites under freeze-thaw cycles [J]. Construction and Building Materials, 2012, 34(3): 522-530.

[21] Lihui Zhang, Liping Guo, Wei Sun. Rheological property and fiber dispersion of high ductility cementitious composites [J]. Journal of Southeast University (Natural Science Edition), 2014, 44(5): 1037-1040.

[22] Xiaoquan Liu. Preparation and performances of high ductility engineered cementitious composites [D].Nanjing: southeast university, 2007.

[23] Shanxi civil science academy and design institute. Standard for test method of basic properties of construction mortar JGJ/T 70-2009 [S]. Beijing: China Architecture & Building Press, 2009.